FEBS Letters 589 (2015) 2186–2193

journal homepage: www.FEBSLetters.org

# Potential regulatory phosphorylation sites in a *Medicago truncatula* plasma membrane proton pump implicated during early symbiotic signaling in roots

Thao T. Nguyen [a,d,1], Jeremy D. Volkening [a,d,1], Christopher M. Rose [b,e], Muthusubramanian Venkateshwaran [c,f], Michael S. Westphall [b,e], Joshua J. Coon [b,e,g], Jean-Michel Ané [c], Michael R. Sussman [a,d,*]

[a] Department of Biochemistry, University of Wisconsin–Madison, Madison, WI 53706, United States
[b] Department of Chemistry, University of Wisconsin–Madison, Madison, WI 53706, United States
[c] Department of Agronomy, University of Wisconsin–Madison, Madison, WI 53706, United States
[d] Biotechnology Center, University of Wisconsin–Madison, Madison, WI 53706, United States
[e] Genome Center of Wisconsin, University of Wisconsin–Madison, Madison, WI 53706, United States
[f] School of Agriculture, University of Wisconsin-Platteville, Platteville, WI 53818, United States
[g] Department of Biomolecular Chemistry, University of Wisconsin–Madison, Madison, WI 53706, United States

ARTICLE INFO

*Article history:*
Received 18 May 2015
Revised 22 June 2015
Accepted 24 June 2015
Available online 17 July 2015

Edited by Julian Schroeder

*Keywords:*
PM $H^+$-ATPase
Proton pump
Nod factor
Phosphorylation
Phosphoproteomics
*Medicago truncatula*

ABSTRACT

**In plants and fungi the plasma membrane proton pump generates a large proton-motive force that performs essential functions in many processes, including solute transport and the control of cell elongation. Previous studies in yeast and higher plants have indicated that phosphorylation of an auto-inhibitory domain is involved in regulating pump activity. In this report we examine the *Medicago truncatula* plasma membrane proton pump gene family, and in particular MtAHA5. Yeast complementation assays with phosphomimetic mutations at six candidate sites support a phosphoregulatory role for two residues, suggesting a molecular model to explain early Nod factor-induced changes in the plasma membrane proton-motive force of legume root cells.**


## 1. Introduction

In animal cells, the primary active transport system across the plasma membrane is a $Na^+/K^+$-ATPase which couples ATP hydrolysis to the efflux of sodium and the influx of potassium ions. Plants and fungi encode a protein with similar overall sequence and structure to the animal enzyme, but instead of moving sodium or potassium it ejects one proton for every ATP molecule hydrolyzed [1–6]. This enzyme, called the plasma membrane (PM) $H^+$-ATPase or proton pump, is encoded by highly conserved gene families in Arabidopsis and rice, two plants for which comprehensive genome-wide sequence analyses are available [7].

The PM proton pump in higher plants and fungi establishes the proton-motive force, comprised of both a membrane potential and a chemical gradient of protons, that powers the uptake of solutes via channels and cotransporters [8,9]. The protein has ten transmembrane domains and a carboxy-terminal auto-inhibitory domain. Current models predict that when residues in this terminal domain are phosphorylated the interaction with, and inhibitory effect on, the ATP-binding catalytic domain is altered [2]. In yeast, for example, supplying glucose to starved cells causes rapid pump activation, and a complex, still unknown orchestration of phosphorylation changes at S911 and T912 of this protein is involved [10].

*Author contributions:* Participated in research design: Nguyen, Volkening, Rose, Venkateshwaran, Westphal, Coon, Ane and Sussman. Conducted experiments: Nguyen, Volkening, Rose, Venkateshwaran. Performed data analysis: Nguyen, Volkening. Wrote or contributed to the writing of the manuscript: Sussman, Volkening, Nguyen, Ane.

* Corresponding author at: UW Biotechnology Center, 425 Henry Mall, Madison, WI 53706, United States. Fax: +1 608 262 6748.
*E-mail address:* msussman@wisc.edu (M.R. Sussman).

[1] These authors contributed equally.

http://dx.doi.org/10.1016/j.febslet.2015.06.035

In higher plants, phosphorylation of the penultimate threonine residue has most often been implicated in this release from inhibition, and a number of effectors and interactions are involved in regulation at this residue [11–15]. In addition, two other regions (R-I and R-II) of the carboxy-terminal tail are also phosphorylated. Depending on the position of the modified residues, pump activity appears to be either positively or negatively regulated [16–19]. There is, however, little certainty on the relative degree of phosphorylation of these domains in situ, nor is there clear data indicating whether there are one or many biochemical mechanisms causing pump activation and inhibition by known environmental effectors (i.e. sugar in yeast and pathogens, cold, hormones, light and salt in plants) [20–22].

The recently sequenced model legume *Medicago truncatula*, a relative of alfalfa, offers the opportunity to perform research using both genetics and biochemistry in the study of the unique symbiotic relationship between nitrogen-fixing rhizobia and their leguminous host plants [23]. Experiments performed over the past decade have indicated that the first step in the development of the symbiotic structures known as root nodules is the recognition by the plant of the presence of rhizobia. This recognition is mediated by diffusible lipochitooligosaccharides (Nod factors) secreted by rhizobia [24]. These compounds are recognized by specific host PM receptor(s) and initiate a protein kinase cascade eventually leading to nodule formation [25]. The nodule is a complex organ that takes several days to form, but rapid changes in membrane transport and cellular morphology are observed in root hairs after Nod factor activation of its PM receptors [26–31]. One of the first observable changes upon activation is an increase in cytoplasmic calcium and proton concentrations, followed by rapid and continuous calcium concentration "spiking" [32–34]. Within the first hour after Nod factor induction, the typical elongated, tapered root hair becomes more bulbous, suggesting substantial changes in turgor pressure, cytoskeletal organization, and PM/cell wall structure [35,36].

In previous work from this group measuring rapid Nod factor-induced changes in the phosphorylome of Medicago [37], we noticed that phosphopeptides from one member of the PM $H^+$-ATPase family displayed significant increases in abundance without a concomitant change in protein concentration, consistent with a predicted increase in catalytic activity. This observation offered an intriguing avenue for future study but the incomplete nature of the Medicago genome sequence and annotations at the time made careful study of this conserved family of proteins difficult. Recently an updated and much improved genome assembly and accompanying annotations were released by the Medicago sequencing consortium [38]. This assembly contained all of our previously identified family members, including ones missing or fragmented in previous genome annotations and found only in scattered data sources, as well as an additional gene located adjacent to a previously annotated locus. In total, 13 family members were located in the Medicago genome, as compared to the 11 found in Arabidopsis and 10 found in rice. In order to facilitate study of specific isoforms, we herein report a comprehensive sequence analysis of those genes, including placement of them in relation to three other model plant species and a re-calculation of tissue-specific expression patterns using published raw data and updated genome annotations. A search of untargeted quantitative data from the Medicago phosphorylome under Nod factor treatment [37] revealed apparent Nod factor-induced increases in serine and threonine phosphorylation in only one of the 13 family members. Phosphorylation changes occurred at six residues located primarily in the carboxy-terminal auto-inhibitory domain. We used yeast complementation assays with phosphomimetic mutations to test the potential regulatory role of these six residues and found that only two are required for optimal functioning of the enzyme expressed in yeast. Taken together, our results provide a plausible molecular mechanism for the increase in plasma membrane proton-motive force that occurs during the very early stages of interaction between leguminous plant roots and their symbiotic rhizobia.

## 2. Materials and methods

### 2.1. Survey of PM $H^+$-ATPases in Medicago truncatula and three other species

Release 4.0 of the *M. truncatula* genome and version 4.0v1 of the JCVI gene annotations were used to search for sequence similarity to a query sequence of Arabidopsis AHA1 using *blastp* (*E*-value cutoff of $1e^{-10}$). The results were manually inspected and a clear delineation of conserved $P_{3A}$-type ATPases from related membrane ATPases was observed. Additional searches of the genome sequence and the TIGR Gene Indices [39] using *tblastn* were used to look for evidence of additional family members – none was found. Similar search parameters were used to identify family members in *Arabidopsis thaliana* (TAIR10), *Oryza sativa* (RGAP7), and *Physcomitrella patens* (v3.0).

### 2.2. Phylogenetic analysis

The 42 protein sequences were aligned using MAFFT v6.864b in local alignment mode (–localpair –maxiterate 1000) [40]. For tree-building, all positions containing gaps in any sequence were removed, with a minimum contiguous length of four, leaving 788 aligned columns. A phylogenetic tree was estimated using PHYML v20111205 with 500 bootstrap iterations [41]. Branches with bootstrap support <300 were collapsed. Physcomitrella proteins PpAHA6 and PpAHA7 were used to root the tree. Tree visualization and final preparation were performed using Archaeopteryx v0.9813 [42].

### 2.3. Analysis of structural conservation

In-house software (available upon request) was used to integrate the full gapped protein multiple alignment with structural annotations for each gene in GFF3 format in order to generate a precisely aligned map of intron positions relative to the aligned amino acid sequences. These positions were used to calculate a simple pairwise distance metric representing conservation of intron number and position. For each pair of sequences $x$ and $y$ in the multiple alignment of length $l$, $x_i$ and $y_i$ represent the presence (1) or absence (0) of an adjacent intron at position $i$. The distance $d$ between them is then calculated as:

$$d = \sum_{i=1}^{l} x_i \oplus y_i$$

Hierarchical clustering with complete linkage was performed in R based on this distance metric.

### 2.4. Tissue-specific gene expression and protein abundance calculations

Raw expression data for *M. truncatula* was derived from two sources but re-analyzed based on up-to-date annotations. Microarray-based expression data for nine tissue types was derived from the experiments performed by Benedito et al. and accessed from the Medicago Gene Expression Atlas (MtGEA) [43,44]. Probe sequences represented on the chip were re-mapped against the Mt4.0v1 transcript sequences using *bwa*

v0.7.10-r789 with a maximum edit distance of one, and probeset IDs were reassigned to the updated gene IDs. For the seven Medicago family members represented on the chip, the minimum probeset specificity was 0.91 and the minimum number of gene-specific probes was 6. These assignments were used to extract normalized expression values from MtGEA.

A second set of Medicago expression data was derived from RNA-Seq experiments performed by Young et al. and included as part of the original Medicago genome publication [23]. For our re-analysis, raw sequencing data from six tissue types (single biological replicates) were retrieved from the NCBI Short Read Archive (study # SRP008485). Reads were adapter-clipped using the *fastx-toolkit* (Hannon lab, Cold Spring Harbor) and gene-level TPM expression estimates were re-calculated using RSEM v1.2.17 [45] based on the Mt4.0v1 transcript set.

Normalized expression data for the Arabidopsis family was extracted from AtGenExpress [46]. RNA-Seq-based expression values for the rice gene family were calculated as described above for Medicago but based on the raw published data in SRA #SRP00882 [47] and mapped against the RGAP7 transcript set.

### 2.5. Read mapping for intron support

For the purposes of evaluating structural annotations, the trimmed data from the RNA-Seq SRA study described above was mapped to the Mt4.0 genome build using the splice-aware software STAR [48]. Intron boundary support was calculated as the count of reads anchored on both adjacent exons and mapping exactly to the intron boundaries. A similar analysis was performed for the rice genes using the SRA dataset from above, resulting in the modification of intron junction positions for four rice genes used in this analysis.

### 2.6. Expression of MtAHA5 in yeast

The *Saccharomyces cerevisiae* strain RS-72 [49] was transformed by the LiAc method [50] and grown on solid selective medium (YNB supplemented with 40 μg/mL adenine, 30 μg/mL histidine, and 2% galactose-SGAH medium) [51]. A single colony was then inoculated in SGAH medium and a serial dilution series was spotted on selective glucose medium (SDAH medium). In RS-72 (*MATa adel-100 his4-519 leu2-3,112 pPMA1:pGAL1*), the endogenous promoter of PM $H^+$-ATPase PMA1 was replaced by the galactose-dependent promoter of GAL1. Wildtype HA-tagged MtAHA5 and its mutant versions were inserted in a centromeric yeast expression vector under control of the PMA1 promoter between *XhoI* and *SpeI* sites of the pMP1745 plasmid [17]. Empty vector pRS315 was transformed in RS72 and used as a negative control.

### 2.7. Site-directed mutagenesis

Mutants were constructed by site-directed mutagenesis using a QuickChange Lightning site-directed mutagenesis kit (Agilent Technologies). All mutated sequences were verified by DNA sequencing.

### 2.8. Yeast complementation assays

After transformation, yeast were used in a growth assay using solid selective glucose SDAH medium at three different pH levels (pH 3.5; pH 4.5; and pH 5.5) to test for the ability of the wild-type MtAHA5 and its mutant derivatives to rescue the yeast *pma1* mutant. This experiment was replicated independently three times with cells from different transformation baths.

### 2.9. Isolation of plasma membrane from transformed yeast

Yeast were grown in selective galactose SGAH medium before inoculating YPD glucose medium for expression of the plant proton pump. The yeast were harvested and membranes were isolated by discontinuous gradient sucrose as previously described [52] except that plasma membranes were resuspended in Pea buffer (0.25 M sucrose, 10 mM KCl, 10 mM HEPES/KOH pH 7.0, 10% glycerol, 1X protease inhibitor cocktail, and 2.5 μg/mL pepstatin A).

### 2.10. SDS-PAGE and Western blotting

Protein concentration was determined using the Quick Start Bradford assay (Biorad) using BSA as the standard. 5 μg of plasma membrane was loaded in each well of a 4–12% Bis-Tris NuPAGE gel (Invitrogen) and subjected to Western blotting using an anti-HA antibody (Covance). The same membrane was then stained with Ponceau-S for use as a loading control.

## 3. Results

### 3.1. Medicago $H^+$-ATPase gene family

A search of the latest Medicago genome build, checked against other existing sources, revealed 13 $P_{3A}$-type plasma membrane $H^+$-ATPase genes, a number generally consistent with the family size in other plant species (11 in Arabidopsis, 10 in rice, 8 in *Physcomitrella patens*). We have proposed a nomenclature for the Medicago gene family similar to that in other model organisms. The names of MtAHA1, MtAHA2, and MtAHA3 have been preserved as previously published [53] and the remaining genes were assigned names MtAHA4 through MtAHA13 based roughly on estimated transcript abundance. The gene symbols for Arabidopsis, rice, and Physcomitrella are as previously published [7,54]. It should be noted that OsAHA8 from rice has been referred to as OsAHA 1 in at least one later paper – here we have kept the original naming [55]. Supplemental Table 1 lists the gene symbols for Medicago, Arabidopsis, rice and Physcomitrella and the corresponding locus accessions used, along with a summary of RNA-Seq-based support for the structural annotations of the Medicago genes.

A multiple alignment of the 42 full-length protein sequences from these species was used to calculate a maximum likelihood phylogeny with bootstrap support $\geqslant 0.6$ (Fig. 1). The Medicago family members can be classified based on this phylogeny into the five subfamilies previously characterized [7]. A second method was also used to examine the evolutionary relationship of these genes based on conservation of gene structure (Supplemental Fig. 1). This type of analysis is not new [3,7], although we have applied a mathematical structure to it not previously used in published work on gene families. These two trees agree closely at the subfamily level and together are suggestive of an evolutionary history. It is clear from the structural tree that PpAHA6 and PpAHA7 are distinct from the rest of the genes surveyed in these four plants, although their protein alignment (as well as a *blastp* search of swissprot) suggests strongly that they are P3A-type ATPases (PpAHA6 shares roughly 69% identity and 82% similarity with PpAHA5, compared to 86%/94% comparing PpAHA5 to its closest match). They both have markedly different intron structure, sharing two introns exactly but with seven "unique" introns (under the assumptions that introns are gained or lost but only rarely "move"). This observation suggests that Physcomitrella retains the descendants of two ancient P3A-type ATPase precursors, one of which went on to form the primary P3A family in modern land plants while the other was apparently lost in angiosperms. The other phylogenetic

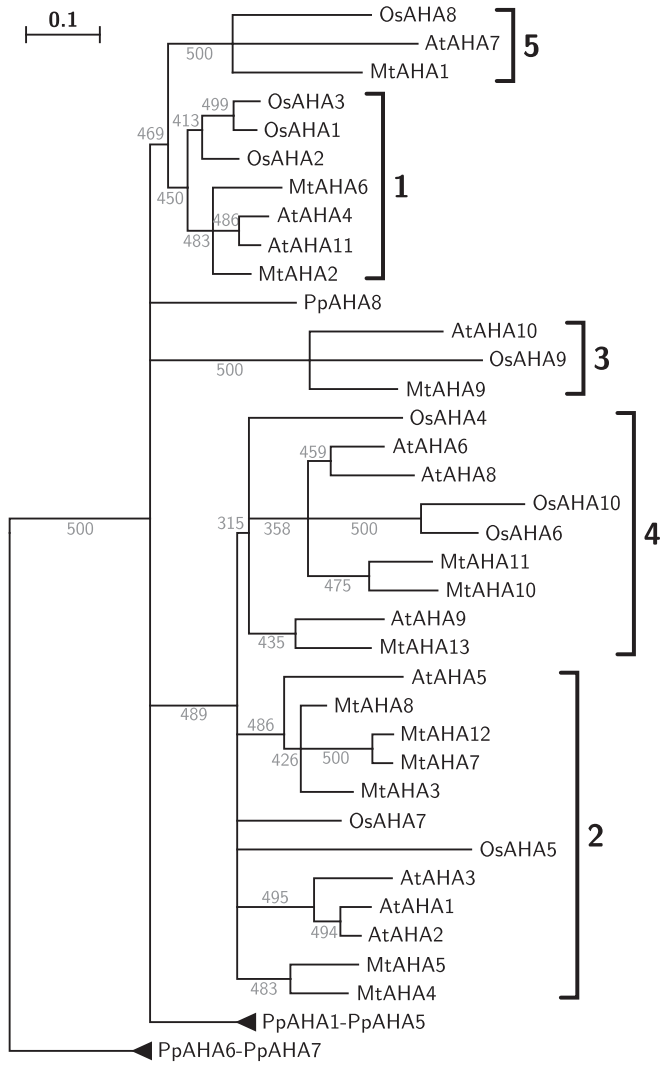


**Fig. 1.** Phylogenetic comparison of 42 protein sequences of $P_{3A}$ $H^+$-ATPase family members from Medicago, Arabidopsis, rice, and Physcomitrella. The tree is rooted using the most distant pump homologs from the model moss *Physcomitrella patens* (*PpAHA6*/*PpAHA7*). The phylogenetic tree was generated using the maximum likelihood method of PHYML with 500 bootstrap replicates. Branches with support values <300/500 were collapsed.

relationships previously described in the $H^+$-ATPases and reinforced here in the protein-based tree are also mirrored in the structural tree. The gene structures suggest a pattern dominated by intron loss as genes and species diverged from ancient precursors. These relationships have been discussed previously [3] and the Medicago gene family fits nicely within this pattern.

### 3.2. Tissue-specific gene expression

A re-examination of gene expression within the families of these four plants based on the latest genome annotations suggested functional conservation as well (Supplemental Figs. 2–5). Previous reviews have suggested only weak correlation between phylogenetic relatedness and tissue-specific expression (3). While it is true that there is little 1:1 correspondence between orthology and expression profile, the untargeted microarray and RNA-Seq datasets examined here suggest broad patterns of shared expression among clades, as well as several observations of specific interest to legume research.

It has already been observed that expression of subfamily 2 members tends to predominate across most tissues. The same is true in Medicago, with MtAHA4 appearing to fill a similar role as AtAHA1 as the most abundantly expressed family member plant-wide. Interestingly, a parallel relationship between AtAHA1/AtAHA2 and MtAHA4/MtAHA5 seems to exist. Both appear to have paralogous relationships, and in both cases one of the genes (AtAHA2, MtAHA5) has taken on a root-centric role (AtAHA2 in Arabidopsis, MtAHA5 in Medicago). Medicago has also undergone greater expansion within subfamily 2 than the other two species.

It has been shown that at least two of the subfamily 5 members are specifically induced during arbuscular mycorrhizal (AM) association and have critical roles in nutrient transport [53,55,56] – baseline expression of this subfamily in most other tissues is low. MtAHA1, the pump seen to be involved in AM symbiosis, does show nodule-specific expression as well in the RNA-Seq dataset, consistent with previous reports of its upregulation in nodulated and AM-associated roots [57,58]. Expression of subfamily 4 members appears to be almost entirely specific to floral tissues. Members of subfamily 3 are not expressed at significant levels in the plants and tissues examined here. Subfamily 1 members have mixed expression patterns. Of note to legume researchers, however, MtAHA6 appears to show some root nodule specificity in both expression datasets.

### 3.3. Phosphorylation sites identified by untargeted mass spectrometry

A large untargeted phosphoproteomics dataset from roots of *M. truncatula* Jemalong A17 treated for one hour with Nod factors isolated from *Sinorhizobium meliloti*, which was generated as part of a previously published study from this group [37] was searched specifically for phosphopeptides from the Medicago PM $H^+$-ATPases. As shown in Table 1, 14 different phosphopeptides derived from the Medicago PM $H^+$-ATPase gene family displaying 10 or more total spectral matches were identified, quantified, and the exact site of modification localized. Although there is considerable biological variability in the data, the only isoform in which phosphopeptide concentrations changed consistently upon Nod factor treatment was MtAHA5. Within that protein, the residues whose level of phosphorylation changed noticeably ($P < 0.15$) by Nod factor treatment included T889, S894, S900, S901 and T957, ranging from a 38% to 86% increase in phosphorylation. These residues are all located near region I of the carboxy terminal tail, and only T889 and S957 are conserved in other proton pump isoforms of Medicago, Arabidopsis and rice (Fig. 2). The amino-terminally localized phosphorylated serine, S10, also showed a change but this was not statistically different from the control. Total protein concentration of MtAHA5 in the same experiment showed no significant change upon treatment, supporting the conclusion that the observed increase in phosphopeptide abundance was due to changes in phosphorylation rather than protein abundance.

### 3.4. Phosphoregulation in yeast

In order to study the possible role of these phosphosites individually, we performed a yeast complementation assay using the RS72 strain [49]. RS72 has a *pma1* mutation in which a galactose-dependent promoter replaces the endogenous promoter, and the yeast are unable to grow in glucose medium alone. In the yeast complementation assay, we used Medicago HA-tagged MtAHA5 and its mutant derivative constructs under PMA1 promoter regulation to test the ability of these various forms of $H^+$-ATPase pump to rescue yeast *pma1* in low-pH medium supplied with glucose.

**Table 1**
Mass spectrometric measurement of the effect of one hour Nod factor treatment on phosphorylation of serine and threonine residues in tryptic peptides isolated from Medicago seedlings. Only phosphopeptides with at least 10 observed spectral matches are shown. Phosphorylated residues are highlighted in bold on the peptide sequences. PSM = peptide spectral match; N = number of observed replicates; SE = standard error. When a peptide is present in more than one protein, the phosphorylated site coordinate represents the location on the first protein listed. Overall protein abundance of MtAHA5 did not change significantly upon treatment (not shown).

| Protein name | Peptide | Phosph. site | PSMs | N | Average ratio (+Nod/−Nod) | SE |
|---|---|---|---|---|---|---|
| MtAHA5 | GSISLDQIKNETVDLER | S10 | 18 | 3 | 1.21 | 0.17 |
| | TLHGLSAPEETSSLFNDK | T889 | 183 | 8 | 1.38 | 0.27 |
| | | S894 | 12 | 4 | 1.86 | 0.67 |
| | | S900 | 10 | 3 | 1.64 | 0.31 |
| | | S901 | 25 | 4 | 1.46 | 0.29 |
| | GLDIETMQQHYTV | T957 | 48 | 7 | 1.43 | 0.23 |
| MtAHA3 | TLHGLQSPDTTNLFNDK | T883 | 27 | 7 | 1.13 | 0.06 |
| | | S889 | 239 | 17 | 1.11 | 0.10 |
| | GLDIDTMQQHYTV | T950 | 15 | 6 | 0.90 | 0.12 |
| MtAHA4 | SISLEQIK | S6 | 149 | 8 | 0.94 | 0.03 |
| | SISLEQIK, SISLEQIKNETVDLER | S8 | 179 | 14 | 1.09 | 0.06 |
| | TLHGLQPPESSGIFNEK | T884 | 378 | 17 | 1.17 | 0.10 |
| | | S894 | 57 | 7 | 1.11 | 0.08 |
| | SSYRELSEIAEQAK | S901 | 11 | 4 | 1.20 | 0.09 |
| | | S902 | 72 | 7 | 1.06 | 0.07 |
| MtAHA3, MtAHA8 | GGISLEEIK | S5 | 114 | 11 | 0.94 | 0.09 |
| MtAHA4, MtAHA8 | GLDIDTIQQHYTV | T951 | 119 | 19 | 1.09 | 0.05 |
| MtAHA2, MtAHA6 | GLDIDTIQQAYTV | T957 | 28 | 18 | 0.98 | 0.07 |
| MtAHA3, MtAHA4, MtAHA5, MtAHA8, MtAHA11, MtAHA13 | GHVESVVK | S933 | 30 | 9 | 0.98 | 0.06 |

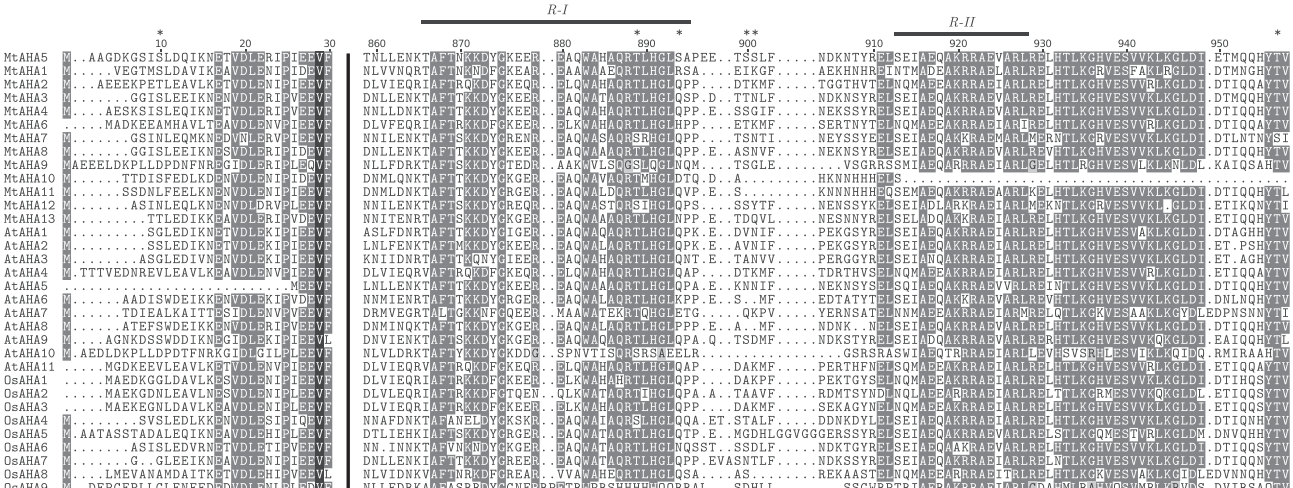


**Fig. 2.** Multiple alignment of $P_{3A}$ $H^+$-ATPase protein family members from Medicago, Arabidopsis, and rice. Shown are N-termini and C-termini numbered based on MtAHA5 coordinates. Asterisks indicate positions of phosphosites tested by yeast complementation. Also shown are the conserved R-I and R-II regulatory domains.

We mutated the six phosphosites of MtAHA5 discussed above either to aspartate (to mimic a negative charge effect of phosphorylation) or to alanine (to mimic the unphosphorylated Ser/Thr). Expression plasmids were transformed into *pma1* yeast and growth was assayed in glucose medium at multiple acidities (Fig. 3). Phosphorylation of the two conserved phosphosites at T889 and T957, which showed increased phosphorylation in response to Nod factor, appears to play an important role in regulation of $H^+$-ATPase activity in yeast, as measured by growth of this fungal line complemented with the plant protein. While T889A MtAHA5 reduced the ability to rescue *pma1* yeast, T889D-transformed yeast showed better growth than wild-type MtAHA5, suggesting that phosphorylation of T889 activates proton pump activity. Both T957A and T957D of MtAHA5 failed to rescue *pma1* yeast, indicating that this threonine is essential for maximal activity of the enzyme. Based on analogy with a number of studies in Arabidopsis, this observation is consistent with the conclusion that the phosphorylation of T957 plays a critical role in regulation of MtAHA5, and that the negative charge of aspartic acid does not sufficiently substitute for the phosphorylated function of this amino acid.

To determine whether phosphorylation alone was responsible for regulation of the plant proton pump activity in yeast, we tested the protein expression of four vectors in yeast cell lines: the transformed wild-type MtAHA5, the mutant T889A (which grew poorly), the mutant T889D (which grew better than wildtype),

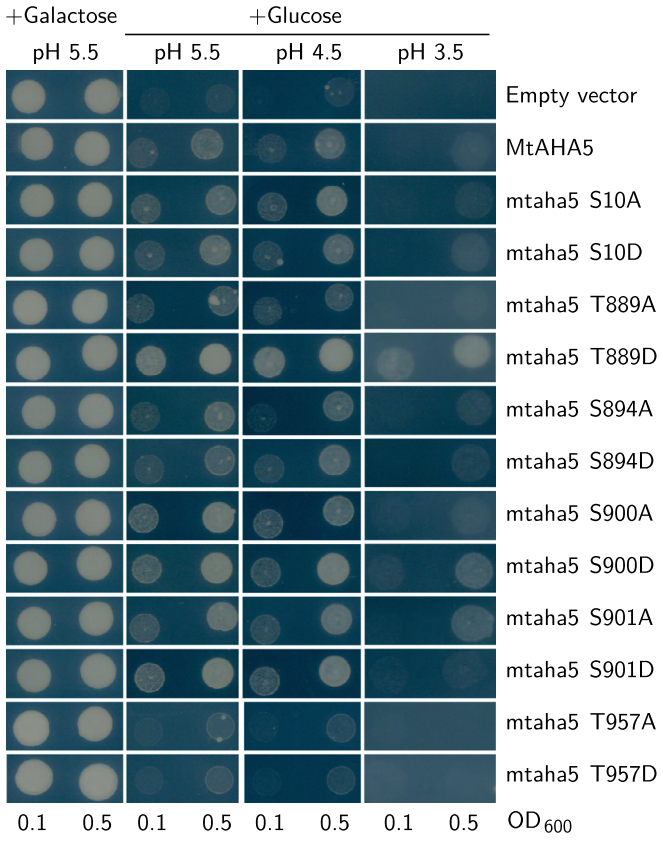


**Fig. 3.** Analysis of phosphosites in Medicago MtAHA5 using complementation assay for yeast *pma1*. The endogenous yeast $H^+$-ATPase PMA1 expressed in RS-72 yeast, when grown in galactose medium, supported cell growth in all strains (furthest left panel). In glucose medium, PMA1 was no longer active – therefore growth corresponds with activity of transformed plant $H^+$-ATPase MtAHA5 under the PMA1 promoter.

and an empty vector control. A Western blot using anti-HA antibody showed little difference in protein level between the wild-type and mutant MtAHA5 (Supplemental Fig. 6). We therefore conclude that changes in yeast growth were due primarily to changes in catalytic activity, rather than concentration, of the proton pump.

Mutation of the other phosphosites (S10, S894, S900, and S901) to either alanine or aspartate did not have any measurable effect on the growth of yeast compared to the wild-type MtAHA5. Phosphorylation at these phosphosites may not play an important role in PM $H^+$-ATPase activity. S894, S900, and S901, which were detected in their phosphorylated form in the untargeted study, are in a variable region and unique to MtAHA5. There is therefore a possibility that they may function in a more specialized fashion. Further *in vivo* studies in plants may be helpful in clarifying the possible function of these phosphosites.

## 4. Discussion

Although there is electrophysiological and biochemical evidence that PM $H^+$-ATPase activity is altered early in the response to cold, salt, pathogens and some growth regulators, and that phosphorylation within a carboxy-terminal domain is involved in regulation, it is still unclear exactly which amino acids in the carboxy tail are the most critical to these responses. In Medicago, previous electrophysiological studies have established that within minutes of Nod factor binding to its PM receptor there is a rapid inhibition of the pump activity followed by a more sustained and larger stimulation over the longer term [28]. In this study we have focused on clarifying the molecular function of changes previously observed in phosphorylation of the pump extracted from tissue treated with and without Nod factors for one hour.

Our observation that the MtAHA5 isoform is the only one whose phosphorylation level is altered by Nod factor treatment in the first hour is consistent with the expression pattern of this gene, which appears almost exclusively in roots and to a small degree in root nodules. Furthermore, the location of phosphorylation changes within the carboxy terminal region is also consistent with prevailing models on how the plant PM $H^+$-ATPase is regulated. Of particular note in these findings is that the changes are not limited to the penultimate threonine, T957, and that changes in four amino acid residues (S894, T889, S900 and S901) located near what has been called Region I, further upstream in the carboxy tail, were observed. Recently published and more comprehensive mass spectral coverage of an Arabidopsis pump has indicated that there are more residues being phosphorylated *in planta* than had previously been recognized [16]. In this respect it is important to note that the 'shotgun' untargeted Medicago study published previously does not provide sufficient amino acid coverage to quantify all possible phosphorylated residues in the pump, and thus we cannot rule out the possibility that there are other amino acids involved in the Nod factor-induced changes in MtAHA5.

The importance of phosphorylation at the penultimate threonine is well-established in Arabidopsis and other systems [12,59,60]. In the absence of fusicoccin, the phosphorylation of this residue is required for 14-3-3 binding and displacement of the C-terminal inhibitory region from the catalytic domain, thus activating the enzyme [12]. To date, the phosphorylation of this threonine has been shown to be increased only in guard cells in response to blue light [61] as well as recently in response to auxin [15] In tobacco, phosphorylation of the penultimate threonine is regulated distinguishably between isoforms. For example, phosphorylation of the penultimate threonine of PMA2 and PMA4 is induced during the exponential stage and reduced during the stationary stage of a cell culture at different rates. In addition, cold stress causes de-phosphorylation of this threonine of PMA4 whereas it has no effect on phosphorylation of PMA4 [22]. It is of value to measure changes in the stoichiometry of phosphorylation and this was achieved in prior work for the penultimate threonine using immunological-based methods for quantifying the phosphorylated and nonphosphorylated modifications at the same specific amino acid [20,22]. Although this can also be achieved using MS/MS procedures, as was shown previously with the AtAHAs from Arabidopsis [9], this requires targeted work using selected reaction monitoring (SRM) on a triple quadrupole MS instrument as well as prefractionation of membranes and/or protein to enrich for the unphosphorylated peptide prior to sample processing. This was not performed in the prior Orbitrap MS instrument-based discovery work with Medicago [37], and thus precise stoichiometric data is not available for this analysis. Here we have used genetic studies to demonstrate that this position in the root-specific MtAHA5 is also important for regulating pump activity.

Phosphorylation of another conserved residue located in the conserved region I, threonine 889, also plays an important role in regulation of MtAHA5. This residue corresponds to T881 of Arabidopsis AHA2 and T889 of tobacco PMA2, and its phosphorylation was reported to regulate enzyme activity in another mechanism different from 14-3-3 binding at the penultimate threonine [18,62]. The phosphorylation of this amino acid decreased in response to the pathogen factor flg22 [63]. Recently, it was reported that T881 of AtAHA2 was phosphorylated *in vitro* by the receptor kinase PSY1R. In response to PSY1 hormone, plant seedlings showed an increase in proton secretion in roots, indicating regulation of plasma membrane proton transport by the receptor

kinase [64]. An opposite effect on AtAHA2 activity was reported for another peptide hormone, RALF. RALF binds to its receptor FERONIA and induces an unknown kinase that phosphorylates AtAHA2 at S899, which in turn reduces activity of AtAHA2 [65]. In this study we showed that phosphomimetic mutants of Thr-889 affect pump activity in yeast and demonstrated the probable role of this residue in activation of the pump following Nod factor signaling.

Recently it was established that a specific member of the plasma membrane pump gene family in Medicago is involved in AM symbiosis and phosphate nutrition [55,56,66], and there is evidence for root nodule expression of this gene as well. It seems reasonable that the evolution of specialized mechanisms that allow legume nodulation has proceeded in a manner such that specialized pump sequences with unique biochemical properties are required in this symbiotic interaction as well. The pump not only plays a major role in establishing the driving force for solute movement across the plasma membrane but evidence suggests it may also play important roles in controlling cell morphology and membrane trafficking early in the response to Nod factors. In future studies it will be of interest to determine whether phosphorylation changes of the root-specific pump MtAHA5 are triggered by fungal mycorrhizal signals as well.

## Acknowledgements

This work was supported by a grant from the National Science Foundation (NSF PGRP No. 0701846) to MRS, JJC, and JMA. CMR was funded by an NSF Graduate Research Fellowship and NIH Traineeship (T32GM008505). TTN and JDV were partially funded by Morgridge Graduate Fellowships. TTN wishes to thank Dr. Miyoshi Haruta for helpful discussions during the course of the project. The authors thank the Town lab at JCVI for access to preliminary genome build data during early stages of the analysis.

## Appendix A. Supplementary data

Supplementary data associated with this article can be found, in the online version, at http://dx.doi.org/10.1016/j.febslet.2015.06.035.

## References

[1] Morsomme, P. and Boutry, M. (2000) The plant plasma membrane $H^+$-ATPase: structure, function and regulation. Biochim. Biophys. Acta 1465, 1–16.
[2] Palmgren, M.G. (2001) Plant plasma membrane $H^+$-ATPases: powerhouses for nutrient uptake. Annu. Rev. Plant Physiol. Plant Mol. Biol. 52, 817–845.
[3] Arango, M., Gevaudant, F., Oufattole, M. and Boutry, M. (2003) The plasma membrane proton pump ATPase: the significance of gene subfamilies. Planta 216, 355–365.
[4] Gaxiola, R.A., Palmgren, M.G. and Schumacher, K. (2007) Plant proton pumps. FEBS Lett. 581, 2204–2214.
[5] Buch-Pedersen, M.J., Pedersen, B.P., Veierskov, B., Nissen, P. and Palmgren, M.G. (2008) Protons and how they are transported by proton pumps. Pflugers Arch. 457, 573–579.
[6] Duby, G. and Boutry, M. (2008) The plant plasma membrane proton pump ATPase: a highly regulated P-type ATPase with multiple physiological roles. Pflugers Arch. 457, 645–655.
[7] Baxter, I., Tchieu, J., Sussman, M.R., Boutry, M., Palmgren, M.G., Gribskov, M., Harper, J.F. and Axelsen, K.B. (2003) Genomic comparison of P-type ATPase ion pumps in Arabidopsis and rice. Plant Physiol. 132, 618–628.
[8] Haruta, M. and Sussman, M.R. (2012) The effect of a genetically reduced plasma membrane protonmotive force on vegetative growth of Arabidopsis. Plant Physiol. 158, 1158–1171.
[9] Haruta, M., Burch, H.L., Nelson, R.B., Barrett-Wilt, G., Kline, K.G., Mohsin, S.B., Young, J.C., Otegui, M.S. and Sussman, M.R. (2010) Molecular characterization of mutant Arabidopsis plants with reduced plasma membrane proton pump activity. J. Biol. Chem. 285, 17918–17929.
[10] Lecchi, S., Nelson, C.J., Allen, K.E., Swaney, D.L., Thompson, K.L., Coon, J.J., Sussman, M.R. and Slayman, C.W. (2007) Tandem phosphorylation of Ser-911 and Thr-912 at the C terminus of yeast plasma membrane $H^+$-ATPase leads to glucose-dependent activation. J. Biol. Chem. 282, 35471–35481.
[11] Fuglsang, A.T., Visconti, S., Drumm, K., Jahn, T., Stensballe, A., Mattei, B., Jensen, O.N., Aducci, P. and Palmgren, M.G. (1999) Binding of 14-3-3 protein to the plasma membrane $H^+$-ATPase AHA2 involves the three C-terminal residues $Tyr^{946}$-Thr-Val and requires phosphorylation of $Thr^{947}$. J. Biol. Chem. 274, 36774–36780.
[12] Svennelid, F., Olsson, A., Piotrowski, M., Rosenquist, M., Ottman, C., Larsson, C., Oecking, C. and Sommarin, M. (1999) Phosphorylation of $Thr^{948}$ at the C terminus of the plasma membrane $H^+$-ATPase creates a binding site for the regulatory 14-3-3 protein. Plant Cell Online 11, 23792392.
[13] Johansson, F., Sommarin, M. and Larsson, C. (1993) Fusicoccin activates the plasma membrane $H^+$-ATPase by a mechanism involving the C-terminal inhibitory domain. Plant Cell 5, 321–327.
[14] Alsterfjord, M., Sehnke, P.C., Arkell, A., Larsson, H., Svennelid, F., Rosenquist, M., Ferl, R.J., Sommarin, M. and Larsson, C. (2004) Plasma membrane $H^+$-ATPase and 14-3-3 isoforms of Arabidopsis leaves: evidence for isoform specificity in the 14-3-3/$H^+$-ATPase interaction. Plant Cell Physiol. 45, 1202–1210.
[15] Spartz, A.K., Ren, H., Park, M.Y., Grandt, K.N., Lee, S.H., Murphy, A.S., Sussman, M.R., Overvoorde, P.J. and Gray, W.M. (2014) SAUR inhibition of PP2C-D phosphatases activates plasma membrane $H^+$-ATPases to promote cell expansion in Arabidopsis. Plant Cell 26, 21292142.
[16] Rudashevskaya, E.L., Ye, J., Jensen, O.N., Fuglsang, A.T. and Palmgren, M.G. (2012) Phosphosite mapping of P-type plasma membrane $H^+$-ATPase in homologous and heterologous environments. J. Biol. Chem. 287, 4904–4913.
[17] Fuglsang, A.T., Guo, Y., Cuin, T.A., Qiu, Q., Song, C., Kristiansen, K.A., Bych, K., Schulz, A., Shabala, S., Schumaker, K.S., Palmgren, M.G. and Zhu, J.-K. (2007) Arabidopsis protein kinase PKS5 inhibits the plasma membrane $H^+$-ATPase by preventing interaction with 14-3-3 protein. Plant Cell 19, 1617–1634.
[18] Piette, A.-S., Derua, R., Waelkens, E., Boutry, M. and Duby, G. (2011) A phosphorylation in the C-terminal auto-inhibitory domain of the plant plasma membrane $H^+$-ATPase activates the enzyme with no requirement for regulatory 14-3-3 proteins. J. Biol. Chem. 286, 18474–18482.
[19] Duby, G., Poreba, W., Piotrowiak, D., Bobik, K., Derua, R., Waelkens, E. and Boutry, M. (2009) Activation of plant plasma membrane $H^+$-ATPase by 14-3-3 proteins is negatively controlled by two phosphorylation sites within the $H^+$-ATPase C-terminal region. J. Biol. Chem. 284, 42134221.
[20] Bobik, K., Boutry, M. and Duby, G. (2010) Activation of the plasma membrane $H^+$-ATPase by acid stress: antibodies as a tool to follow the phosphorylation status of the penultimate activating Thr. Plant Signal. Behav. 5, 681–683.
[21] Yang, Y., Qin, Y., Xie, C., Zhao, F., Zhao, J., Liu, D., Chen, S., Fuglsang, A.T., Palmgren, M.G., Schumaker, K.S., Deng, X.W. and Guo, Y. (2010) The Arabidopsis chaperone J3 regulates the plasma membrane $H^+$-ATPase through interaction with the PKS5 kinase. Plant Cell 22, 13131332.
[22] Bobik, K., Duby, G., Nizet, Y., Vandermeeren, C., Stiernet, P., Kanczewska, J. and Boutry, M. (2010) Two widely expressed plasma membrane $H^+$-ATPase isoforms of Nicotiana tabacum are differentially regulated by phosphorylation of their penultimate threonine. Plant J. 62, 291–301.
[23] Young, N.D., Debelle, F., Oldroyd, G.E.D., Geurts, R., Cannon, S.B., Udvardi, M.K., Benedito, V.A., Mayer, K.F.X., Gouzy, J., Schoof, H., de Peer, Y.V., Proost, S., Cook, D.R., Meyers, B.C., Spannagl, M., Cheung, F., Mita, S.D., Krishnakumar, V., Gundlach, H., Zhou, S., Mudge, J., Bharti, A.K., Murray, J.D., Naoumkina, M.A., Rosen, B., Silverstein, K.A.T., Tang, H., Rombauts, S., Zhao, P.X., Zhou, P., Barbe, V., Bardou, P., Bechner, M., Bellec, A., Berger, A., Berges, H., Bidwell, S., Bisseling, T., Choisne, N., Couloux, A., Denny, R., Deshpande, S., Dai, X., Doyle, J.J., Dudez, A.-M., Farmer, A.D., Fouteau, S., Franken, C., Gibelin, C., Gish, J., Goldstein, S., Gonzalez, A.J., Green, P.J., Hallab, A., Hartog, M., Hua, A., Humphray, S.J., Jeong, D.-H., Jing, Y., Jocker, A., Kenton, S.M., Kim, D.-J., Klee, K., Lai, H., Lang, C., Lin, S., Macmil, S.L., Magdelenat, G., Matthews, L., McCorrison, J., Monaghan, E.L., Mun, J.-H., Najar, F.Z., Nicholson, C., Noirot, C., O'Bleness, M., Paule, C.R., Poulain, J., Prion, F., Qin, B., Qu, C., Retzel, E.F., Riddle, C., Sallet, E., Samain, S., Samson, N., Sanders, I., Saurat, O., Scarpelli, C., Schiex, T., Segurens, B., Severin, A.J., Sherrier, D.J., Shi, R., Sims, S., Singer, S.R., Sinharoy, S., Sterck, L., Viollet, A., Wang, B.-B., Wang, K., Wang, M., Wang, X., Warfsmann, J., Weissenbach, J., White, D.D., White, J.D., Wiley, G.B., Wincker, P., Xing, Y., Yang, L., Yao, Z., Ying, F., Zhai, J., Zhou, L., Zuber, A., Denarie, J., Dixon, R.A., May, G.D., Schwartz, D.C., Rogers, J., Quetier, F., Town, C.D. and Roe, B.A. (2011) The Medicago genome provides insight into the evolution of rhizobial symbioses. Nature 480, 520–524.
[24] Denarie, J., Debelle, F. and Prome, J.-C. (1996) Rhizobium lipo-chitooligosaccharide nodulation factors: signaling molecules mediating recognition and morphogenesis. Annu. Rev. Biochem. 65, 503–535.
[25] Venkateshwaran, M., Ane, J., 2011. The Molecular and physiological basis of nutrient use efficiency in crops. In: Hawkesford, M.J., Barraclough, P. (eds.). Wiley-Blackwell, Oxford, UK, 457–489.
[26] Ehrhardt, D.W., Atkinson, E.M. and Long, S.R. (1992) Depolarization of alfalfa root hair membrane potential by Rhizobium meliloti Nod factors. Science 256, 998–1000.
[27] Felle, H.H., Kondorosi, E., Kondorosi, A. and Schultze, M. (1995) Nod signal-induced plasma membrane potential changes in alfalfa root hairs are differentially sensitive to structural modifications of the lipochitooligosaccharide. Plant J. 7, 939–947.
[28] Felle, H.H., Kondorosi, E., Kondorosi, A. and Schultze, M. (1996) Rapid alkalinization in alfalfa root hairs in response to rhizobial lipochitooligosaccharide signals. Plant J. 10, 295–301.
[29] Felle, H.H., Kondorosi, E., Kondorosi, A. and Schultze, M. (1998) The role of ion fluxes in Nod factor signalling in Medicago sativa. Plant J. 13, 455–463.

[30] Cardenas, L., Holdaway-Clarke, T.L., Sanchez, F., Quinto, C., Feijo, J.A., Kunkel, J.G. and Hepler, P.K. (2000) Ion changes in legume root hairs responding to Nod factors. Plant Physiol. 123, 443–452.
[31] Kurkdjian, A., Bouteau, F., Pennarun, A.-M., Convert, M., Cornel, D., Rona, J.-P. and Bousquet, U. (2000) Ion currents involved in early Nod factor response in Medicago sativa root hairs: a discontinuous single-electrode voltage-clamp study. Plant J. 22, 9–17.
[32] Ehrhardt, D.W., Wais, R. and Long, S.R. (1996) Calcium spiking in plant root hairs responding to Rhizobium nodulation signals. Cell 85, 673–681.
[33] Felle, H.H., Kondorosi, E., Kondorosi, A. and Schultze, M. (1999) Elevation of the cytosolic free [$Ca^{2+}$] is indispensable for the transduction of the Nod factor signal in alfalfa. Plant Physiol. 121, 273–280.
[34] Geurts, R. and Bisseling, T. (2002) Rhizobium Nod factor perception and signalling. Plant Cell 14 (Suppl.), S239–S249.
[35] Miller, D.D., Klooster, H.B.L. and Emons, A.M.C. (2000) Lipochito-oligosaccharide nodulation factors stimulate cytoplasmic polarity with longitudinal endoplasmic reticulum and vesicles at the tip in vetch root hairs. Mol. Plant Microbe Interact. 13, 1385–1390.
[36] Esseling, J.J., Lhuissier, F.G.P. and Emons, A.M.C. (2003) Nod factor-induced root hair curling: continuous polar growth towards the point of Nod factor application. Plant Physiol. 132, 1982–1988.
[37] Rose, C.M., Venkateshwaran, M., Volkening, J.D., Grimsrud, P.A., Maeda, J., Bailey, D.J., Park, K., Howes-Podoll, M., den Os, D., Yeun, L.H., Westphall, M.S., Sussman, M.R., Ane, J.-M. and Coon, J.J. (2012) Rapid phosphoproteomic and transcriptomic changes in the rhizobia-legume symbiosis. Mol. Cell. Proteomics 11, 724–744.
[38] Tang, H., Krishnakumar, V., Bidwell, S., Rosen, B., Chan, A., Zhou, S., Gentzbittel, L., Childs, K.L., Yandell, M., Gundlach, H., Mayer, K.F., Schwartz, D.C. and Town, C.D. (2014) An improved genome release (version Mt4.0) for the model legume Medicago truncatula. BMC Genomics 15, 312.
[39] Quackenbush, J., Cho, J., Lee, D., Liang, F., Holt, I., Karamycheva, S., Parvizi, B., Pertea, G., Sultana, R. and White, J. (2001) The TIGR Gene Indices: analysis of gene transcript sequences in highly sampled eukaryotic species. Nucleic Acids Res. 29, 159–164.
[40] Katoh, K., Misawa, K., Kuma, K. and Miyata, T. (2002) MAFFT: a novel method for rapid multiple sequence alignment based on fast Fourier transform. Nucleic Acids Res. 30, 3059–3066.
[41] Guindon, S., Dufayard, J.-F., Lefort, V., Anisimova, M., Hordijk, W. and Gascuel, O. (2010) New algorithms and methods to estimate maximum-likelihood phylogenies: assessing the performance of PhyML 3.0. Syst. Biol. 59, 307–321.
[42] Han, M.V. and Zmasek, C.M. (2009) PhyloXML: XML for evolutionary biology and comparative genomics. BMC Bioinformatics 10, 356.
[43] Benedito, V.A., Torres-Jerez, I., Murray, J.D., Andriankaja, A., Allen, S., Kakar, K., Wandrey, M., Verdier, J., Zuber, H., Ott, T., Moreau, S., Niebel, A., Frickey, T., Weiller, G., He, J., Dai, X., Zhao, P.X., Tang, Y. and Udvardi, M.K. (2008) A gene expression atlas of the model legume Medicago truncatula. Plant J. 55, 504–513.
[44] He, J., Benedito, V.A., Wang, M., Murray, J.D., Zhao, P.X., Tang, Y. and Udvardi, M.K. (2009) The Medicago truncatula gene expression atlas web server. BMC Bioinformatics 10, 441.
[45] Li, B. and Dewey, C.N. (2011) RSEM: accurate transcript quantification from RNA-Seq data with or without a reference genome. BMC Bioinformatics 12, 323.
[46] Schmid, M., Davison, T.S., Henz, S.R., Pape, U.J., Demar, M., Vingron, M., Scholkopf, B., Weigel, D. and Lohmann, J.U. (2005) A gene expression map of Arabidopsis thaliana development. Nat. Genet. 37, 501–506.
[47] Davidson, R.M., Gowda, M., Moghe, G., Lin, H., Vaillancourt, B., Shiu, S.-H., Jiang, N. and Robin Buell, C. (2012) Comparative transcriptomics of three Poaceae species reveals patterns of gene expression evolution. Plant J. Cell Mol. Biol. 71, 492–502.
[48] Dobin, A., Davis, C. A., Schlesinger, F., Drenkow, J., Zaleski, C., Jha, S., Batut, P., Chaisson, M., Gingeras, T.R., 2012. STAR: ultrafast universal RNA-seq aligner. Bioinformatics, bts635.
[49] Cid, A., Perona, R. and Serrano, R. (1987) Replacement of the promoter of the yeast plasma membrane ATPase gene by a galactose-dependent promoter and its physiological consequences. Curr. Genet. 12, 105–110.
[50] Gietz, R.D. and Schiestl, R.H. (2007) High-efficiency yeast transformation using the LiAc/SS carrier DNA/PEG method. Nat. Protoc. 2, 31–34.
[51] Regenberg, B., Villalba, J.M., Lanfermeijer, F.C. and Palmgren, M.G. (1995) C-terminal deletion analysis of plant plasma membrane $H^+$-ATPase: yeast as a model system for solute transport across the plant plasma membrane. Plant Cell 7, 1655–1666.
[52] Panaretou, B. and Piper, P. (2006) Isolation of yeast plasma membranes. Methods Mol. Biol. 313, 27–32.
[53] Krajinski, F., Hause, B., Gianinazzi-Pearson, V. and Franken, P. (2002) Mtha1, a plasma membrane $H^+$-ATPase gene from Medicago truncatula, shows arbuscule-specific induced expression in mycorrhizal tissue. Plant Biol. 4, 754–761.
[54] Okumura, M., Takahashi, K., Inoue, S. and Kinoshita, T. (2012) Evolutionary appearance of the plasma membrane $H^+$-ATPase containing a penultimate threonine in the bryophyte. Plant Signal. Behav. 7, 979–982.
[55] Wang, E., Yu, N., Bano, S.A., Liu, C., Miller, A.J., Cousins, D., Zhang, X., Ratet, P., Tadege, M., Mysore, K.S., Downie, J.A., Murray, J.D., Oldroyd, G.E.D. and Schultze, M. (2014) A $H^+$-ATPase that energizes nutrient uptake during mycorrhizal symbioses in rice and Medicago truncatula. Plant Cell 26, 1818–1830.
[56] Krajinski, F., Courty, P.-E., Sieh, D., Franken, P., Zhang, H., Bucher, M., Gerlach, N., Kryvoruchko, I., Zoeller, D., Udvardi, M. and Hause, B. (2014) The $H^+$-atpase HA1 of Medicago truncatula is essential for phosphate transport and plant growth during arbuscular mycorrhizal symbiosis. Plant Cell 26, 1808–1817.
[57] Manthey, K., Krajinski, F., Hohnjec, N., Firnhaber, C., Puhler, A., Perlick, A.M. and Kuster, H. (2004) Transcriptome profiling in root nodules and arbuscular mycorrhiza identifies a collection of novel genes induced during Medicago truncatula root endosymbioses. Mol. Plant. Microbe Interact. 17, 1063–1077.
[58] Benedito, V.A., Li, H., Dai, X., Wandrey, M., He, J., Kaundal, R., Torres-Jerez, I., Gomez, S.K., Harrison, M.J., Tang, Y., Zhao, P.X. and Udvardi, M.K. (2010) Genomic inventory and transcriptional analysis of Medicago truncatula transporters. Plant Physiol. 152, 1716–1730.
[59] Robertson, W.R., Clark, K., Young, J.C. and Sussman, M.R. (2004) An Arabidopsis thaliana plasma membrane proton pump is essential for pollen development. Genetics 168, 1677–1687.
[60] Maudoux, O., Batoko, H., Oecking, C., Gevaert, K., Vandekerckhove, J., Boutry, M. and Morsomme, P. (2000) A plant plasma membrane $H^+$-ATPase expressed in yeast is activated by phosphorylation at its penultimate residue and binding of 14-3-3 regulatory proteins in the absence of fusicoccin. J. Biol. Chem. 275, 17762–17770.
[61] Kinoshita, T. and Shimazaki, K. (1999) Blue light activates the plasma membrane $H^+$-ATPase by phosphorylation of the C-terminus in stomatal guard cells. EMBO J. 18, 5548–5558.
[62] Niittyla, T., Fuglsang, A.T., Palmgren, M.G., Frommer, W.B. and Schulze, W.X. (2007) Temporal analysis of sucrose-induced phosphorylation changes in plasma membrane proteins of Arabidopsis. Mol. Cell. Proteomics MCP 6, 1711–1726.
[63] Nuhse, T.S., Bottrill, A.R., Jones, A.M.E. and Peck, S.C. (2007) Quantitative phosphoproteomic analysis of plasma membrane proteins reveals regulatory mechanisms of plant innate immune responses. Plant J. Cell Mol. Biol. 51, 931–940.
[64] Fuglsang, A.T., Kristensen, A., Cuin, T.A., Schulze, W.X., Persson, J., Thuesen, K.H., Ytting, C.K., Oehlenschlaeger, C.B., Mahmood, K., Sondergaard, T.E., Shabala, S. and Palmgren, M.G. (2014) Receptor kinase-mediated control of primary active proton pumping at the plasma membrane. Plant J. 80, 951–964.
[65] Haruta, M., Sabat, G., Stecker, K., Minkoff, B.B. and Sussman, M.R. (2014) A peptide hormone and its receptor protein kinase regulate plant cell expansion. Science 343, 408–411.
[66] Hubberten, H.-M., Sieh, D., Zoller, D., Hoefgen, R., Krajinski, F., 2015. *Medicago truncatula* Mthal-2 mutants lose metabolic responses to mycorrhizal colonization. Plant Signal. Behav. [online]. doi:http://dx.doi.org/10.4161/15592324.2014.989025.